pH-induced folding of an apoptotic coiled coil

KAUSHIK DUTTA, ANDREI ALEXANDROV, HE HUANG, AND STEVEN M. PASCAL

Department of Biochemistry and Biophysics, University of Rochester Medical Center, Rochester, New York 14642, USA

(RECEIVED July 18, 2001; FINAL REVISION September 18, 2001; ACCEPTED September 19, 2001)

Abstract

Par-4 is a 38-kD protein pivotal to the apoptotic pathways of various cell types, most notably prostate cells and neurons, where it has been linked to prostate cancer and various neurodegenerative disorders including Alzheimer's and Huntington's diseases and HIV encephalitis. The C-terminal region of Par-4 is responsible for homodimerization and the ability of Par-4 to interact with proposed effector molecules. In this study, we show that the C-terminal 47 residues of Par-4 are natively unfolded at physiological pH and temperature. Evidence is rapidly accumulating that natively unfolded proteins play an important role in various cellular functions and signaling pathways, and that folding can often be induced on complexation with effector molecules or alteration of environment. Here we use primarily CD studies to show that changes in the environment, particularly pH and temperature, can induce the Par-4 C terminus to form a self-associated coiled coil.

Keywords: Leucine zipper; coiled coil; apoptosis; circular dichroism; protein folding; natively unfolded

Supplemental material: See www.proteinscience.org.

The Par-4 protein was first identified by differential screening for upregulated genes in prostate cancer cells undergoing apoptosis (Sells et al. 1994). Par-4 expression has since been detected in diverse tissue types (Boghaert et al. 1997), and its upregulation in neurons has been linked to a variety of neurodegenerative disorders, including Alzheimer's (Guo et al. 1998), Huntington's (Duan et al. 2000), and Parkinson's (Mattson et al. 1999) diseases, HIV encephalitis (Kruman et al. 1999), and amylotrophic lateral sclerosis (Pedersen et al. 1999). Downregulation of Par-4 has been linked to several cancers, including those of the prostate (Sells et al. 1994, 1997), colon (Zhang and DuBois 2000), and kidney (Cook et al. 1999). The primary sequence of the Par-4 protein contains a heptad repeat at the C terminus, which strongly indicates the presence of an LZ, and is essential for the ability of Par-4 to lower the apoptotic threshold of cells (Sells et al. 1997), as well as for the ability of Par-4 to self-associate and interact with various proposed effector molecules (Diaz-Meco et al. 1996; Johnstone et al. 1996; Page et al. 1999). For instance, the LZ domain has been shown to bind to the zinc-coordinating regulatory domain of two atypical isoforms of PKC (Diaz-Meco et al. 1996). The resulting downregulation of aPKC activity has been proposed as the pathway through which Par-4 induces increased sensitivity to apoptotic stimuli (Diaz-Meco et al. 1996). Various other interactions have been investigated to further elucidate the role of Par-4 in apoptosis and cancer, resulting in linkage of Par-4 to Bcl-2, NF-κB/IF-κB (Diaz-Meco et al. 1999; Qiu et al. 1999a; Camandola and Mattson 2000), and the Ras oncogene pathway (Barradas et al. 1999; Nalca et al. 1999; Qiu et al. 1999b).

Reprint requests to: Kaushik Dutta and Steven M. Pascal, Department of Biochemistry and Biophysics, University of Rochester Medical Center, Box 712, 601 Elmwood Avenue, Rochester, NY 14642; e-mail: kaushik_dutta@urmc.rochester.edu; pascal@oxbow.biophysics.rochester.edu; fax: (716) 275-6007.

Abbreviations: Par-4, prostate apoptosis response protein number 4; LZ, leucine zipper; PKC, protein kinase C; aPKC, atypical protein kinase C; MBP, maltose-binding protein; CD, circular dichroism; $[\Theta]$, molar ellipticity; $[\Theta_{222}]$, molar ellipticity at 222 nm; $[\Theta_D]$, molar ellipticity at 222 nm at the low pH limit; $[\Theta_M]$, molar ellipticity at 222 nm at the high pH limit; n, Hill coefficient; T_m, characteristic melting temperature; f_M, fractional population of monomer state; K_d, dissociation constant; C_{tot}, total concentration of peptide; ΔH_m, enthalpy of melting; ΔC_p, change in heat capacity at constant pressure; $[\Theta_{D0}]$, molar ellipticity at 222 nm at the low pH limit extrapolated to 0 K; γ, constant describing the slope of $[\Theta_D]$ versus temperature; $[\Theta_{208}]$, molar ellipticity at 208 nm; WT1, Wilm's tumor protein; Dlk, DAP-like kinase.

Article and publication are at http://www.proteinscience.org/cgi/doi/10.1101/ps.28801.

Two features of the primary sequence of the Par-4 C terminus (Fig. 1) are immediately evident. The first is the preponderance of polar residues (33 of 47), particularly those of acidic character (14 of 47). This type of amino acid distribution has been linked to the phenomenon of "natively unfolded" proteins, which lack stable conformational order under "physiological" conditions (for recent reviews, see Wright and Dyson 1999; Uversky et al. 2000). The second feature is the presence of a heptad repeat indicative of a coiled-coil structure, as shown via the helical wheel representation in Figure 1.

Here we show that a peptide representing the Par-4 C terminus is natively unfolded at physiological pH and temperature, but can be induced to form a coiled coil at low pH and low temperature. Salt helps to stabilize the coiled coil at high pH, but is destabilizing at low pH, and the two-state conformational equilibrium is also affected by peptide concentration. These observations are discussed through an analysis of the primary sequence of the Par-4 LZ domain. These results indicate that changes in cellular environment, particularly pH, could affect not only Par-4 folding, but also interactions of Par-4 with effector molecules.

Results

The thick trace in Figure 2A shows the CD spectrum of the Par-4 LZ in 12 mM NaP_i, 20 mM NaCl (pH 6.5) at 25°C.

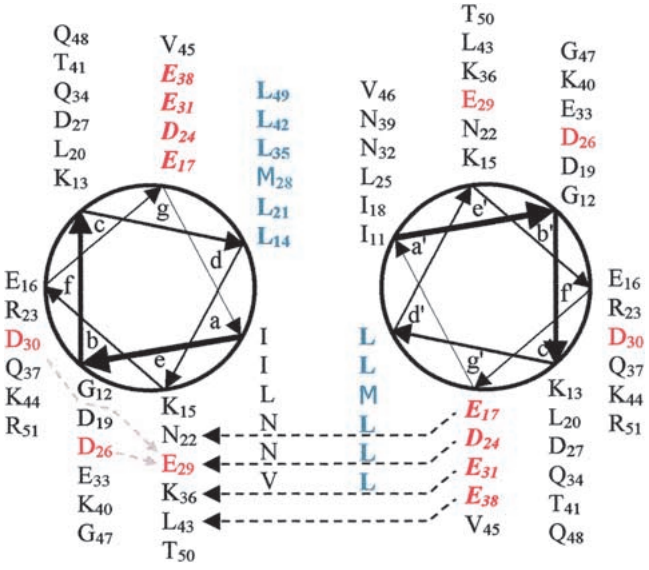

Fig. 1. Helical wheel representation of residues 11–51 of the Par-4 LZ peptide. Positions in the heptad repeat are denoted by *abcdefg*. The leucine repeat at the *d* position is shown in blue, and the acidic repeat at the *g* position is in red italics. The potential $g' \rightarrow e$ interactions involving the acidic g' repeat are shown as dark dashed arrows. Lighter dashed arrows indicate possible intramolecular charge–charge repulsions involving E29. The 51-amino acid peptide used in this study contains the C-terminal 47 residues of Par-4 (residues 286–332) preceded by a 4-residue cloning artifact.

This spectrum represents an ~82% random coil structure (~18% helical). On lowering the temperature to −5°C (Fig. 2A, bottom trace), the helical content is increased to 41%, with the appearance of minima near 222 nm and 208 nm. The isodichroic point near 203 nm, which has been seen in the study of other LZs, is commonly taken as evidence of a two-state transition (Krylov et al. 1994; Kohn et al. 1995; Jelesarov et al. 1998). Taken together, the data of Figure 2A indicate an equilibrium between a nonfolded state and a marginally more stable helical state, which becomes somewhat increasingly favored at lower temperature.

To further investigate the conformational variability, we took CD spectra over a range of pH values, with the temperature fixed at 5°C (Fig. 2B). The data indicate that acidic pH stabilizes helix formation. Fractional helicity increases from ~24% to 75% between pH 8.5 and pH 5.5. Next, the temperature was once again varied, but this time with the pH fixed at 5.75 (Fig. 2C). Lower temperature favors helix formation more markedly at this pH (compare Fig. 2A), with fractional helicity increasing from ~17% to 86% as the temperature decreases from 45°C to 0°C. Again, isodichroic points near 203 nm in Figure 2B and 2C indicate a two-state transition.

Plots of $[\Theta_{222}]$ versus pH at 11 different temperatures are shown in Figure 2D. Note that data were not acquired below pH 5.5 because of reduced peptide solubility. The data at each temperature were fit to equation 1 (see Materials and Methods) to yield values of the conformational pKa, which is the characteristic pH at the transition midpoint, and the Hill coefficient, indicating the degree of cooperativity. Results are tabulated in Table 1, and pKa values are depicted graphically in the Figure 2D inset. Fitting at higher temperatures requires considerable extrapolation, and results in large uncertainties. Therefore, these values are not plotted in the inset. However, it is clear that, at least at low temperature, the apparent pKa decreases in a regular fashion as temperature increases, and the Hill coefficients of ~2 imply cooperative folding as a function of pH.

Plots of $[\Theta_{222}]$ versus temperature in 20 mM NaCl at five different pH values are shown in Figure 2E. The values of T_m and ΔH_m, the characteristic melting temperature and the enthalpy of melting, were extracted as described in Materials and Methods. The results are shown in Supplemental Material, Table 1, along with similar results for two other salt concentrations. T_m decreases from ~35 °C to −1 °C as the pH increases from 5.5 to 8.0 (Fig. 2E, inset). The decrease of T_m with pH is very steep at pH 6 and below, and flattens out somewhat at high pH, where titration of acidic groups should be complete. Note though that fitting is less reliable at high pH.

The conformation is also sensitive to salt concentration. Figure 2F shows the variation in fractional helicity as a function of pH, at three different NaCl concentrations at 5°C. At pH 8.5, 20 mM NaCl results in only 13% helical

content, whereas increasing NaCl concentration to 80 or 140 mM increases the helical content to ~22%. The situation is reversed at pH 5.5, where 20 and 80 mM salt induces 80% helix, and increasing the salt concentration to 140 mM decreases the helical content to 70%. The data were fit to equation 1 in an analogous manner as the curves from Figure 2D, with fractional helicity replacing molar ellipticity. The resulting pKa values are in the range of 6.14 ± 0.05 for each salt concentration, which is consistent with the values extracted for the 5°C curve of Figure 2D (Table 1). The Hill coefficients are again near 2, although the value for the 20 mM NaCl curve is 2.86 ± 0.35, and the Hill coefficients for the 80 mM and 140 mM NaCl curves fall just below 2. Thus it appears that low salt may marginally increase the cooperativity of the transition. It should be noted that the increase in the calculated cooperativity is correlated with the wider disparity between the plateau values of fractional helicity at 20 mM NaCl. Thermal stability, as measured by T_m, appears to follow a similar trend (Supplemental Material, Table 1), with high salt somewhat favoring helix formation at high pH, and low salt marginally stabilizing at low pH.

The concentration dependence of the Par-4 peptide conformation was also investigated. At each of the three pH values represented in Figure 3, increased peptide concentration resulted in increased thermal stability (increased T_m). T_m values for pH 6.5 were extracted at higher concentrations, because extraction of T_m values at low concentration and high pH is inherently inaccurate (see Fig. 2E, top two curves). Note that $1/T_m$ as a function of $\ln(C_{tot})$ is approximately linear (Fig. 3 inset), consistent with a two-state transition at each pH value (Marky and Breslauer 1987; Jelesarov and Bosshard 1996).

Discussion

Coiled coils are amphipathic helical oligomerization motifs found in many types of proteins (Lupas 1996, 1997; Hicks et al. 1997). In naturally occurring dimeric forms, two α-helices coil around each other with a slight left-handed superhelical twist. The amino acid sequence can be organized into a seven-residue repetitive heptad pattern, designated $(abcdefg)_n$, in which *a* and *d* positions are generally hydrophobic and are present at the center of the oligomeric interface. The most common hydrophobic residues at these positions are Leu, Val, and Ile. Coiled coils with predominantly Leu at position *d* are known as LZs. Asn is also quite common at the *a* position, and its presence has been correlated with the occurrence of a parallel dimeric state (Harbury et al. 1993; Potekhin et al. 1994; Lumb and Kim 1995a; Gonzalez et al. 1996a,b,c; Zeng et al. 1997). The solvent-exposed *b*, *c*, and *f* positions affect stability, solubility, and the specificity of interactions with other molecules, but are not generally thought to affect the fold or interhelical orientation as strongly as the *a*, *d*, *e*, and *g* residues (O'Neil and DeGrado 1990; Dahiyat et al. 1997; Spek et al. 1998).

Although hydrophobic interactions at the oligomeric interface are the principal driving force for folding and oligomerization of coiled coils, electrostatic interactions can also contribute significantly to stability and instability. For instance, charged side chains in the *e* and *g* positions can interact with the opposite strands (g' and e', respectively). These interactions can be complementary or noncomplementary, depending on the type of residues present at the *e* and *g* positions. Although questions remain regarding the contributions to stability from complementary interactions, it is clear that charge clashes such as between two acidic side chains can have a profound affect on both the stability and stoichiometry of coiled coils (Krylov et al. 1994, 1998; Zhou et al. 1994; Kohn et al. 1995, 1997; Jelesarov and Bosshard 1996; Lavigne et al. 1996; Durr et al. 1999).

The present studies were conducted with a 51-residue peptide, representing the C-terminal 47 residues of Par-4 (residues 286–332) preceded by a 4-residue cloning artifact. For simplicity, these residues have been redesignated residues 1–51. Residues 11–51 are depicted in helical wheel format in Figure 1. Orienting the heptad repeat by placing the leucine repeat at the *d* position results in an additional hydrophobic repeat at the *a* position, with the exception of two Asn residues, which indicate the presence of a parallel coiled-coil dimer structure. The distribution of Leu predominantly at *d* and Ile at *a* also indicates a propensity to form a dimeric coiled coil, whereas reversal of this pattern would be consistent with tetrameric coil formation (Harbury et al. 1993). Our experimental results are consistent with these sequence-based predictions, although the oligomeric state and interhelical orientation have not been determined explicitly. The experimental evidence for environment-dependent coiled-coil formation is discussed in the following sections.

Helicity, two-state cooperative transition, $[\Theta_{222}]/[\Theta_{208}]$

CD spectra indicate that the PAR-4 LZ peptide forms a predominantly α helical structure at low pH and low temperature (Fig. 2B and 2C, lower traces). Although this alone is not sufficient to specify a coiled coil, conformationally stable isolated helices in aqueous solution are rare in the absence of helix-favoring conditions such as less polar solvents (Dyson et al. 1988; Saudek et al. 1991). It is well known that in coiled coils, helix formation and interhelical assembly are commonly tightly coupled, and the presence of isolated helices is rarely detected (Ozeki et al. 1991; Wendt et al. 1995; Zitzewitz et al. 1995; Sosnick et al. 1996; Wendt et al. 1997; Jelesarov et al. 1998). The folding pathway therefore represents an equilibrium between just two predominant states: the unfolded monomer and the coiled-

coil dimer, with no detectable intermediate. Thus, evidence of a two-state transition is further evidence of coiled-coil formation. As noted previously, the isodichroic points near 203 nm in Figure 2 A–C are characteristic of a two-state transition, and further support is supplied by the ability to fit the curves of Figure 2 D–F with a two-state model (see Materials and Methods). The Hill coefficients of these curves indicate that the transition is cooperative. Note also that $[\Theta_{222}]$ becomes more negative than $[\Theta_{208}]$ at maximal helicity (Fig. 2B and 2C, lower traces). The value of the $[\Theta_{222}]$ /$[\Theta_{208}]$ ratio for noncoiled helices is typically near 0.83. For α helices that are part of a coiled-coil structure, the

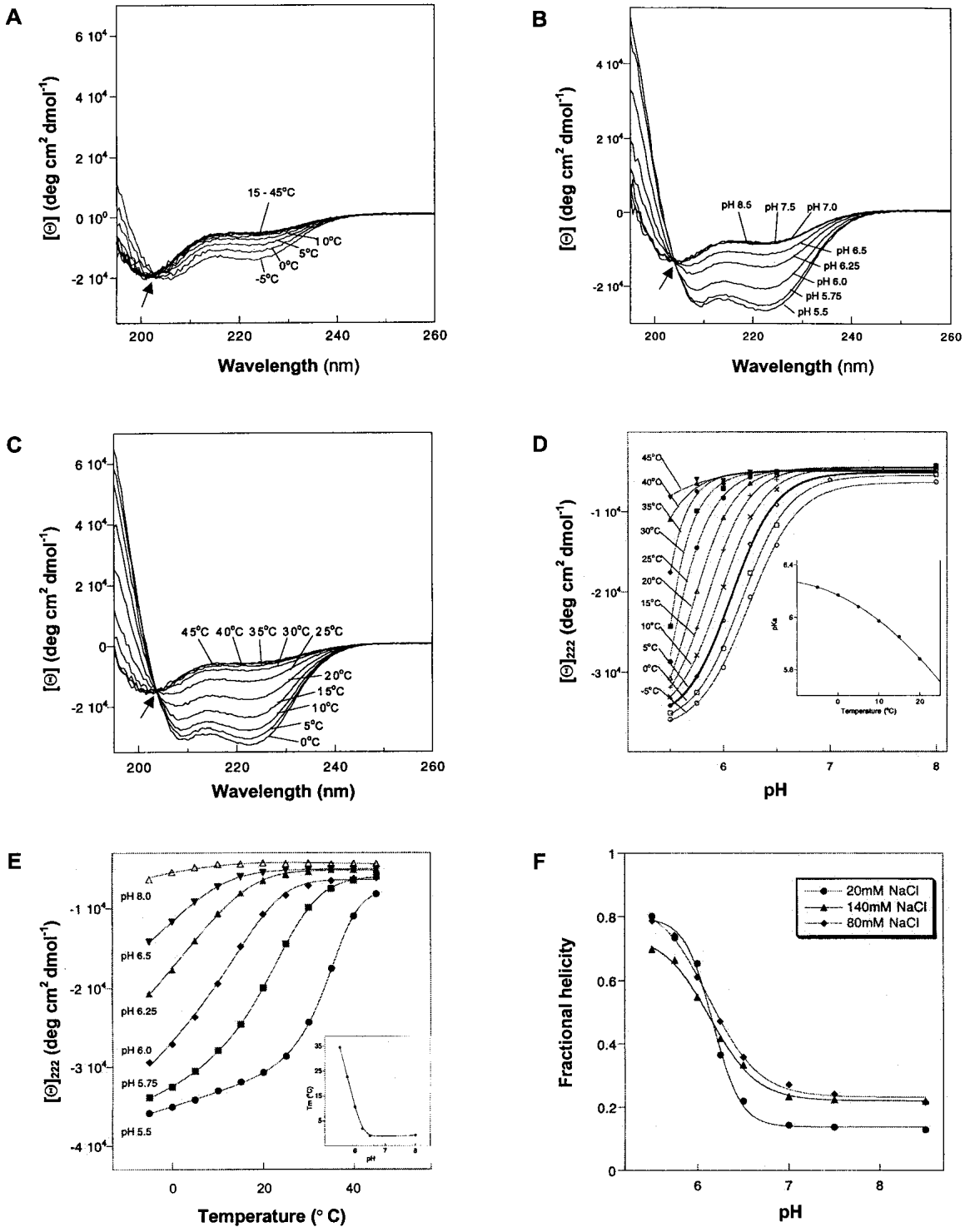

Fig. 2

Table 1. *pKa and Hill coefficients extracted by fitting the curves from Figure 2D to the modified Henderson-Hasselbalch equation (equation 1)*

Temp. (°C)	pKa	Hill coefficient
−5	6.23 ± 0.02	1.88 ± 0.17
0	6.17 ± 0.02	1.95 ± 0.17
5	6.08 ± 0.02	2.04 ± 0.15
10	5.97 ± 0.02	2.10 ± 0.15
15	5.85 ± 0.02	2.22 ± 0.13
20	5.69 ± 0.03	2.15 ± 0.17
25	5.41 ± 0.14	2.02 ± 0.41
30	5.47 ± 0.50	2.22 ± 1.40
35	5.51 ± 0.84	2.55 ± 3.30

parallel polarized amide π–π* transition becomes less dichroic, effectively reducing the negativity of $[\Theta_{208}]$. Because $[\Theta_{222}]$ is unaffected, the $[\Theta_{222}]/[\Theta_{208}]$ ratio increases to ~1.03. Hence the $[\Theta_{222}]/[\Theta_{208}]$ ratios of ~1.08 and 1.06 (bottom traces of Fig. 2B and 2C, respectively) are further confirmation of helical supercoiling (Muhle-Goll et al. 1994; Zhou et al. 1994; Lavigne et al. 1995).

Dependence on concentration, pH, and salt

The concentration dependence of T_m shown in Figure 3 is a strong indication of intermolecular interactions, and is not consistent with the formation of noninteracting monomeric helices. The linearity seen in the inset graph is consistent with a two-state transition. The pH dependence is also consistent with coiled-coil formation. In addition to a leucine repeat at position *d*, the sequence of the Par-4 LZ peptide has a strong acidic repeat at position *g*. In Figure 1, the two helical wheels have been aligned in a parallel symmetric fashion. Characteristically, parallel dimeric coiled-coil side chains in the *g* position make interhelical contact with *e′* side chains at the i + 5 position (for instance, E17′ with N22; also E17 with N22′, where the prime indicates the second helical molecule). The role of polar interhelical contacts in coiled-coil formation and stability has been much discussed (Krylov et al. 1994, 1998; Zhou et al. 1994; Kohn et al. 1995, 1997; Jelesarov and Bosshard 1996; Lavigne et al. 1996; Durr et al. 1999). Although the importance of complementary (e.g., E31–K36′) and neutral (e.g., E17′–N22 or E38′–L43) interactions appears to be case dependent, negative–negative interactions such as D24′–E29 have a considerable destabilizing affect on helix formation. In the present case, it is likely that charge–charge repulsion between D24′and E29 (and the symmetric D24–E29′ repulsion) is a major factor in disfavoring coiled-coil formation at high pH (Fig. 2B). However, it should also be noted that amino acids in position *e* of coiled coils have been shown to interact intramolecularly with the *b*, *c*, *d*, and *f* residues of the same heptad. Similarly, the *g* position residues interact intramolecularly with the *d* and *f* positions of the same heptad, and the *a* and *d* residues of the next heptad (Marti et al. 2000). Thus, several intramolecular complimentary charge–charge interactions are expected to occur on coil formation, including K15–E16, D24–R23, and K36–E33. Intramolecular negative–negative charge clashes include E17–E16, E31–D30, E29–D26, and E29–D30. The involvement of E29 in one interchain and two intrachain repulsions (a total of six repulsions in a symmetric dimer) indicate that this residue is key to the pH-dependent folding of the Par-4 LZ, although each of the earlier listed contacts could contribute to helical instability at high pH.

Decrease in pH has been shown to increase the helicity of acidic coiled coils, presumably due to at least partial protonation of one or more of the offending acidic side chain groups (Zhou et al. 1994; Jelesarov et al. 1998; Krylov et al. 1998; Durr et al. 1999). Although the pKa of an acidic side chain normally falls in the 4.0–4.5 range, in a local environment containing other acidic groups, the pKa may increase. More specifically, the pKa values of acidic side chains involved in *e–g* charge clashes in coiled coils have been shown to be elevated (Anderson et al. 1990; Yang et al. 1993; Lumb and Kim 1995b). This preferential protonation would abrogate the charge repulsion and allow the now neutral side chain to contribute to the stability of the hydrophobic core. The altered single group pKa values can be reflected in the conformational pKa, although the exact nature of the correspondence has been difficult to establish. The conformational pKa values found here (Fig. 2D) are consistent with this explanation.

The salt dependence shown in Figure 2F further supports the importance of charge–charge interactions in the folding

Fig. 2. CD spectroscopy and thermodynamic analysis of Par-4 LZ peptide. (*A*) Far ultraviolet (UV) CD spectra as a function of temperature in 12 mM NaP_i and 20 mM NaCl (pH 6.5). The thick trace was recorded at 25°C. Peptide concentration was 22 μM. (*B*) Far UV CD spectra as a function of pH in 12 mM NaP_i and 140 mM NaCl at 5°C. Peptide concentration was 22 μM. (*C*) Far UV CD spectra as a function of temperature in 12 mM NaP_i and 20 mM NaCl (pH 5.75). Peptide concentration was 27 μM. Isodichroic points near 203 nm in (*A–C*) are identified by arrows. (*D*) pH dependence of the molar ellipticity $[\theta]_{222}$ as a function of temperature. These curves were fit to a modified Henderson–Hasselbalch equation (equation 1) to extract the conformational pKa (*inset*) and Hill coefficient as functions of temperature (Table 1). Sample was 18 μM peptide in 12 mM NaP_i and 20 mM NaCl. (*E*) Temperature dependence of the molar ellipticity $[\theta]_{222}$ as a function of pH. These curves were fit as described in the text (equations 2–6) to extract the T_m (*inset*) and ΔH_m as functions of pH (Supplemental Material, Table 1). Sample was 18 μM peptide in 12 mM NaP_i and 20 mM NaCl. (*F*) The fractional helicity versus pH at three different salt concentrations. Sample was 27 μM peptide in 12mM NaP_i, 5°C.

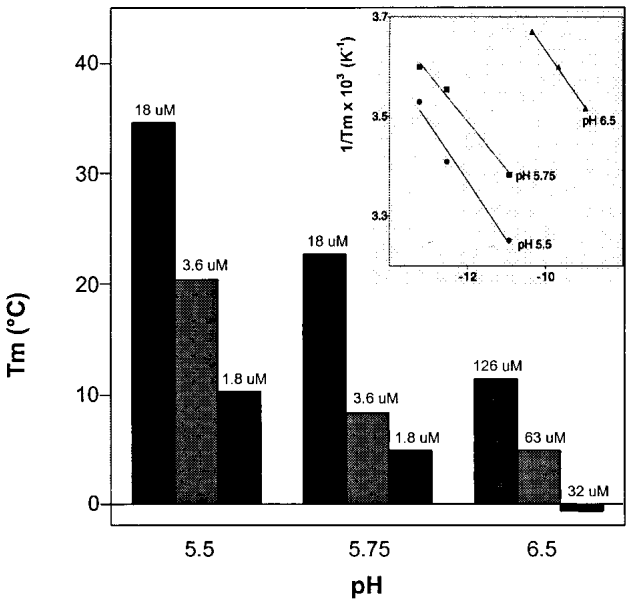

Fig. 3. Variation of T_m versus total PAR-4 LZ concentration (labeled above each bar) at three different pH values. $1/T_m$ versus natural log of concentration (Ctot) is plotted in the *inset*. Buffer was 12 mM NaP_i and 20 mM NaCl.

of the Par-4 LZ. At high pH, the most influential charge effects are the noncomplementary contacts: intermolecularly between D24′ and E29 (also D24–E29′), and the intramolecular negative–negative clashes noted earlier. Increased salt concentration can help to screen the effects of these clashes, either by providing local counter ions or by increasing the dielectric constant of the medium (Goto et al. 1990; Kohn et al. 1997). Accordingly, increasing salt concentration appears to increase helicity slightly. At low pH, one or more of the repulsive interactions has been reduced by at least partial protonation of one or more of the acidic groups. However, the complementary charge interactions, such as E31′–K36 may still be active, because pKa values of acidic residues involved in stabilizing or marginally destabilizing interactions have been shown to be reduced or only slightly elevated (Anderson et al. 1990; Yang et al. 1993; Lumb and Kim 1995b). Thus, at low pH, increasing salt concentration may affect the complementary interactions more prominently. This effect could also be described as an increase in desolvation penalty when the medium has a higher dielectric constant (Hendsch and Tidor 1999). It should be noted, however, that NaCl can have many and varied effects in solution, including salting out, which is widely recognized as a cause of protein and peptide aggregation and precipitation, but which can also simply encourage hydrophobic contacts to form at the dimer interface (Leberman and Soper 1995; Kohn et al. 1997). This effect might tend to be more pronounced at low pH, because the dimer interface will be less charged. It is also possible that the relatively minor salt dependence could simply be due to a slightly different helical orientation in different ionic environments rather than an actual difference in helical content. These and other effects must be carefully balanced to obtain a more complete picture of the effects of salt, pH, temperature, concentration, and intrachain and interchain ionic effects on coiled-coil formation.

Par-4 function

The Par-4 LZ region is required not only for homodimerization, but also for interaction with proposed effector molecules (see Introduction). It is through these interactions that Par-4 is thought to sensitize cells to apoptotic stimuli. But how does this natively unfolded region interact with effector proteins? The answer is far from certain, but discussion will serve to introduce several possibilities.

First, the concentration dependence of the Par-4 LZ conformation may play a role. Higher Par-4 concentrations in the cell could lead to a higher proportion of dimerization. Indeed, overexpression of Par-4 does enhance the potency of apoptotic stimuli in cells where Par-4 is normally expressed at lower levels (Boghaert et al. 1997), although this effect can also be explained without resort to increased dimerization percentages. Second, other regions of the Par-4 molecule may influence the conformation of the C terminus. For instance, the N-terminal regions of two Par-4 molecules may interact in a manner insufficient to provide the driving force for dimerization in the absence of the LZ region, but with sufficient affinity to stabilize the C-terminal coil. Alternatively, the N-terminal region may form a surface that favors and therefore stabilizes the folded conformation of the LZ region.

Third, effector molecules may be attracted to the unstructured acidic tail of Par-4, and the LZ may be induced to fold only after complexation, or as part of the binding event. Examples of induced fold have been observed in many types of proteins, including those involved in transcriptional activation (Kussie et al. 1996; Radhakrishnan et al. 1997, 1998), RNA binding (Tan and Frankel 1994; Puglisi et al. 1995; Battiste et al. 1996), and cell-cycle progression (Kriwacki et al. 1996; Pavletich 1999). Formation of a heterodimeric zipper from a Par-4 molecule and a partner molecule is one type of induced fold that should be considered. Along these lines, model acidic LZ peptides, which were conformationally unstable due to anionic repulsions, have been shown to form stable heterodimeric zippers with basic LZ peptides at neutral pH, when the charge complementarity at the *e* and *g* positions was optimally designed (Jelesarov and Bosshard 1996). Complementary heterodimerization has also been observed with naturally occurring LZ sequences, such as Max/Myc (Lavigne et al. 1995, 1998) and Jun/Fos (O'Shea et al. 1989). In fact, because attractive charge–charge interactions do not appear to be as important as the absence of repulsive interactions, a

LZ peptide with simply an absence of acidic residues in the *e* position may be capable of heterodimerizing with the PAR-4 C terminus.

To date, interactions have not been detected between the Par-4 LZ and LZ regions of other proteins. The proposed cellular targets for the Par-4 LZ include the zinc-binding domains of the aPKCs and WT1, and an arginine-rich region of Dlk/ZIP kinase (Kogel et al. 1998; Kawai et al. 1998). The name of the latter kinase denotes the predicted presence of a C-terminal leucine zipper (ZIP), which mediates interaction with LZ-containing transcription factors such as ATF-4 (Kawai et al. 1998), but does not appear to be responsible for interaction with Par-4 (Page et al. 1999). However, we find that the Par-4 interacting region of ZIP kinase also possesses coiled-coil propensity (~75% probability, as predicted by the program Multicoil (Wolf et al. 1997)). This region may play the role of a basic LZ and heterodimerize with the PAR-4 LZ, or may interact in another manner, due at least in part to charge complementarity.

Finally, exposure to an altered cellular or subcellular pH environment may help to stabilize the homodimeric coiled coil. The correlation between reduction of intracellular pH and the onset of apoptosis is an area of intense investigation (for a recent review, see Matsuyama and Reed 2000). The pH-induced folding of proteins such as Par-4 may play a role in this process. As for local pH environment, it is interesting to note that in contrast to other PKC isoforms, strong evidence has been presented for subcellular localization of the aPKCs to lysosome-targeted endosomes (Sanchez et al. 1998). The nearby acidic environment of the endosomal interior (pH ~ 5.0) would be ideal for self-association of the Par-4 LZ, although aPKCs are generally assumed to tether to the outer endosomal membrane, and we are not aware of any evidence for translocation of Par-4 or any of its binding partners to the endosomal interior. We were unable to gather CD data for the Par-4 LZ at pH 5.0 as a result of solubility constraints, but conservative extrapolation of the inset plot in Figure 2E using a sigmoidal function predicts a T_m of 42 ± 4 °C (pH 5.0). Because folding as a function of temperature becomes increasingly cooperative at low pH (compare pH 6.25 and pH 5.5 curves in Fig. 2E), a T_m of 42°C together with the projected shape of a pH 5.0 melting curve predicts a predominantly folded state at 37°C. Thus, if it were to translocate into the endosomal compartment, Par-4 would be strongly self-associated, and would present a nearly fully folded coiled coil for interaction with potential binding partners. Precedent exists for pH-induced folding and interactions in the endosomal environment: pH-dependent coiled-coil formation of the influenza hemagglutinin protein in an endosomal environment has been linked to membrane fusion events critical for viral infection (Carr and Kim 1993; Bullough et al. 1994; Weissenhorn et al. 1997; Chen et al. 1999).

We have shown that the conformation of a peptide representing the Par-4 C-terminus exists in an equilibrium between an intrinsically unstructured monomer and a coiled coil. The unfolded monomer predominates under typical physiological conditions, but the coiled coil becomes favored at low pH and low temperature. Salt and peptide concentration also affect the equilibrium. In a cellular environment, the Par-4 LZ conformation could become increasingly favored on interaction with other molecules, other regions of the Par-4 molecule, or on exposure to a reduced pH environment.

Materials and methods

Protein expression and purification

The Par-4 LZ, comprising residues 286–332 of racine Par-4, was subcloned into the H-MBP-3C vector (Alexandrov et al. 2001). Following previously described expression and purification of the resulting MBP-fusion protein and fusion cleavage with recombinant protease (Alexandrov et al. 2001), the eluted Par-4 protein was dialyzed against an aqueous buffer containing 12 mM NaP_i (pH 7.5). An additional ion exchange purification step was performed with a Hi-Trap Q Sepharose column (Amersham-Pharmacia). The protein was eluted with an increasing NaCl gradient, and exchanged into aqueous buffer containing 20 mM NaCl and 12 mM NaP_i (pH 6.5). SDS-PAGE and MALDI mass spectroscopy showed the protein to be >99% pure. The amino acid composition was confirmed and the concentration was determined by amino acid analysis.

CD spectroscopy

CD spectra were recorded on an AVIV model 202 CD spectrometer equipped with a thermoelectric sample temperature controller and a 0.1-cm path length cuvette. Spectra were recorded in 0.5-nm steps from 260 to 190 nm with an integration time of 2 sec at each wavelength, and baseline corrected against a cuvette containing buffer alone. Estimates of the fractional helicity were made using either $[\Theta_{222}]/-35{,}000$ (Chen et al. 1974) or the SELCON program (Seerama and Woody 1993), which analyzes CD spectra for α-helical, β-sheet and other content (includes random coil and turn conformations), using a database of spectra from 48 proteins of known secondary structure. These two methods agree to within 5% for all studies reported here, and so are not distinguished in the discussions . Thermal stability was determined by monitoring the molar ellipticity at 222 nm as a function of temperature at 5°C intervals with 5 min equilibration and a collection time of 30 sec at each temperature. No significant irreversibility of CD spectra was detected when temperature, pH, salt concentration, or peptide concentration was cycled, provided that peptide precipitation at low pH was avoided.

Extraction of thermodynamic parameters via nonlinear least square best fitting of a two-state model (two unfolded monomers ↔ folded dimer) closely followed the work of Bosshard and colleagues (Jelesarov and Bosshard 1996; Durr et al. 1999; Marti et al. 2000). Variation of molar ellipticity and fractional helicity with pH was used to extract values of the conformational pKa and the Hill coefficient (n), at various temperatures and salt con-

centrations, via a modified form of the Henderson–Hasselbalch equation:

$$[\Theta]_{obs} = \frac{[\Theta_D] + [\Theta_M]10^{n(pH-pKa)}}{1 + 10^{n(pH-pKa)}} \quad (1)$$

where the known variables are the observed molar ellipticity at 222 nm ($[\Theta]_{obs}$) and the pH. Fitting also yielded the values of $[\Theta_D]$ and $[\Theta_M]$, the extrapolated plateau values of molar ellipticity at 222 nm at the acidic and basic pH limits (where the subscript denotes dimer or monomer).

Variation of molar ellipticity with temperature was used to extract values of T_m and ΔH_m at five different pH values, three different salt concentrations, and various peptide concentrations via the following procedure:

The observed molar ellipticity can be related to the plateau values by:

$$[\Theta]_{obs} = f_M[\Theta_M] + (1 - f_M)[\Theta_D] \quad (2)$$

where f_M is the fractional population of the monomer state. Equation 2 can be rearranged to:

$$f_M = \frac{[\Theta]_{obs} - [\Theta_D]}{[\Theta_M] - [\Theta_D]} \quad (3)$$

By definition, $K_d = [M]^2/[D]$, $[M] = f_M C_{tot}$, and $[D] = C_{tot}(1-f_M)/2$, and thus:

$$K_d = \frac{2f_M{}^2 C_{tot}}{1 - f_M} \quad (4)$$

where K_d is the dissociation constant, and C_{tot} is the total peptide concentration. Equation 4 can be solved for f_M via the quadratic equation:

$$f_M = \frac{-K_d + \sqrt{K_d{}^2 + 8C_{tot}K_d}}{4C_{tot}} \quad (5)$$

Equation 5 can be rendered into a useful form by substituting the expression for f_M from equation 3, and also substituting the following expression for K_d, which assumes that ΔC_p, the change in heat capacity, is much less than ΔH_m (Jelesarov and Bosshard 1996; Durr et al. 1999; Marti et al. 2000):

$$K_d = C_{tot} \exp\left[\frac{\Delta H_m}{R}\left(\frac{1}{T_m} - \frac{1}{T}\right)\right] \quad (6)$$

After the temperature dependence of $[\Theta_D]$ is introduced by substituting $[\Theta_D] = [\Theta_{D0}] + \gamma T$, the modified equation 5 can be solved for $[\Theta]_{obs}$ and then used to fit experimental melting curves such as those shown in Figure 2E. Extracted parameters include T_m, ΔH_m, $[\Theta_{D0}]$, $[\Theta_M]$, and the constant γ.

Electronic supplemental material

Supplemental material includes a table of extracted thermodynamic parameters from fitting curves such as in Figure 2E via equations 2–6, at three different salt concentrations, six different pH values, and several Par-4 concentrations.

Acknowledgments

This work was supported by U.S. Army Prostate Cancer Research Program award number DAMD17–98–1–8551 (to S.M.P.). The authors thank Stephen Sells, Vivek Rangnekar, Maria Diaz-Meco, Jorge Moscat, Kara Bren, Satoshi Ohnishi, Yaqiong Lin, and Snehal Pandya.

The publication costs of this article were defrayed in part by payment of page charges.This article must therefore be hereby marked "advertisement" in accordance with 18 USC section 1734 solely to indicate this fact.

References

Alexandrov, A., Dutta, K., and Pascal, S.M. 2001. MBP-fusion with a viral protease cleavage site: One-step cleavage/purification of insoluble proteins. *Biotechniques* **30:** 1194–1198.

Anderson, D.E., Becktel, W.J., and Dahlquist, F.W. 1990. pH-induced denaturation of proteins: A single salt bridge contributes 3–5 kcal/mol to the free energy of folding of T4 lysozyme. *Biochemistry* **29:** 2403–8.

Barradas, M., Monjas, A., Diaz-Meco, M.T., Serrano, M., and Moscat, J. 1999. The downregulation of the pro-apoptotic protein Par-4 is critical for Ras-induced survival and tumor progression. *EMBO J.* **18:** 6362–9.

Battiste, J.L., Mao, H.Y., Rao, N.S., Tan, R.Y., Muhandiram, D.R., Kay, L.E., Frankel, A.D., and Williamson, J.R. 1996. α helix-RNA major groove recognition in an HIV-1 Rev peptide RRE RNA complex. *Science* **273:** 1547–1551.

Boghaert, E.R., Sells, S.F., Walid, A.J., Malone, P., Williams, N.M., Weinstein, M.H., Strange, R., and Rangnekar, V.M. 1997. Immunohistochemical analysis of the proapoptotic protein Par-4 in normal rat tissues. *Cell Growth Differ.* **8:** 881–90.

Bullough, P.A., Hughson, F.M., Skehel, J.J., and Wiley, D.C. 1994. Structure of influenza haemagglutinin at the pH of membrane fusion. *Nature* **371:** 37–43.

Camandola, S. and Mattson, M.P. 2000. Pro-apoptotic action of PAR-4 involves inhibition of NF-κB activity and suppression of BCL-2 expression. *J. Neurosci. Res.* **61:** 134–9.

Carr, C.M. and Kim, P.S. 1993. A spring-loaded mechanism for the conformational change of influenza hemagglutinin. *Cell* **73:** 823–32.

Chen, J., Skehel, J.J., and Wiley, D.C. 1999. N- and C-terminal residues combine in the fusion-pH influenza hemagglutinin HA(2) subunit to form an N cap that terminates the triple-stranded coiled coil. *Proc.Natl. Acad. Sci.* 96: 8967–72.

Chen, Y.J., Yang, K., and Chan, K. 1974. Determination of the helix and β form of proteins in aqueous solution by circular dichroism. *Biochemistry* **13:** 3350–3359.

Cook, J., Krishnan, S., Ananth, S., Sells, S.F., Shi, Y., Walther, M.M., Linehan, W.M., Sukhatme, V.P., Weinstein, M.H., and Rangnekar, V.M. 1999. Decreased expression of the pro-apoptotic protein Par-4 in renal cell carcinoma. *Oncogene* **18:** 1205–8.

Dahiyat, B.I., Gordon, D.B., and Mayo, S.L. 1997. Automated design of the surface positions of protein helices. *Protein Sci.* **6:** 1333–7.

Diaz-Meco, M.T., Municio, M.M., Frutos, S., Sanchez, P., Lozano, J., Sanz, L., and Moscat, J. 1996. The product of par-4, a gene induced during apoptosis, interacts selectively with the atypical isoforms of protein kinase C. *Cell* **86:** 777–86.

Diaz-Meco, M.T., Lallena, M.J., Monjas, A., Frutos, S., and Moscat, J. 1999. Inactivation of the inhibitory κB protein kinase/nuclear factor κB pathway by Par-4 expression potentiates tumor necrosis factor α-induced apoptosis. *J. Biol. Chem.* **274:** 19606–12.

Duan, W., Guo, Z., and Mattson, M.P. 2000. Participation of par-4 in the degeneration of striatal neurons induced by metabolic compromise with 3-nitropropionic acid. *Exp. Neurol.* **165:** 1–11.

Durr, E., Jelesarov, I., and Bosshard, H.R. 1999. Extremely fast folding of a very stable leucine zipper with a strengthened hydrophobic core and lacking electrostatic interactions between helices. *Biochemistry* **38:** 870–80.

Dyson, H.J., Rance, M., Houghten, R.A., Wright, P.E., and Lerner, R.A. 1988. Folding of immunogenic peptide fragments of proteins in water solution. II. The nascent helix. *J. Mol. Biol.* **201:** 201–17.

Gonzalez Jr., L., Brown, R.A., Richardson, D., and Alber, T. 1996a. Crystal structures of a single coiled-coil peptide in two oligomeric states reveal the basis for structural polymorphism. *Nat. Struct. Biol.* **3:** 1002–9.

Gonzalez Jr., L., Plecs, J.J., and Alber, T. 1996b. An engineered allosteric switch in leucine-zipper oligomerization. *Nat. Struct. Biol.* **3:** 510–5.
Gonzalez Jr., L., Woolfson, D.N., and Alber, T. 1996c. Buried polar residues and structural specificity in the GCN4 leucine zipper. *Nat. Struct. Biol.* **3:** 1011–8.
Goto, Y., Calciano, L.J., and Fink, A.L. 1990. Acid-induced folding of proteins. *Proc. Natl. Acad. Sci.* **87:** 573–577.
Guo, Q., Fu, W., Xie, J., Luo, H., Sells, S.F., Geddes, J.W., Bondada, V., Rangnekar, V.M., and Mattson, M.P. 1998. Par-4 is a mediator of neuronal degeneration associated with the pathogenesis of Alzheimer disease. *Nat. Med.* **4:** 957–62.
Harbury, P.B., Zhang, T., Kim, P.S., and Alber, T. 1993. A switch between two-, three-, and four-stranded coiled coils in GCN4 leucine zipper mutants. *Science* **262:** 1401–1407.
Hendsch, Z.S. and Tidor, B. 1999. Electrostatic interactions in the GCN4 leucine zipper: substantial contributions arise from intramolecular interactions enhanced on binding. *Protein Sci.* **8:** 1381–92.
Hicks, M.R., Holberton, D.V., Kowalczyk, C., and Woolfson, D.N. 1997. Coiled-coil assembly by peptides with non-heptad sequence motifs. *Fold. Des.* **2:** 149–58.
Jelesarov, I. and Bosshard, H.R. 1996. Thermodynamic characterization of the coupled folding and association of heterodimeric coiled coils (leucine zippers). *J. Mol. Biol.* **263:** 344–58.
Jelesarov, I., Durr, E., Thomas, R.M., and Bosshard, H.R. 1998. Salt effects on hydrophobic interaction and charge screening in the folding of a negatively charged peptide to a coiled coil (leucine zipper). *Biochemistry* **37:** 7539–50.
Johnstone, R.W., See, R.H., Sells, S.F., Wang, J., Muthukkumar, S., Englert, C., Haber, D.A., Licht, J.D., Sugrue, S.P., Roberts, T., Rangnekar, V.M., and Shi, Y. 1996. A novel repressor, par-4, modulates transcription and growth suppression functions of the Wilms' tumor suppressor WT1. *Mol. Cell. Biol.* **16:** 6945–56.
Kawai, T., Matsumoto, M., Takeda, K., Sanjo, H., and Akira, S. 1998. ZIP kinase, a novel serine/threonine kinase which mediates apoptosis. *Mol. Cell. Biol.* **18:** 1642–51.
Kogel, D., Plottner, O., Landsberg, G., Christian, S., and Scheidtmann, K.H. 1998. Cloning and characterization of Dlk, a novel serine/threonine kinase that is tightly associated with chromatin and phosphorylates core histones. *Oncogene* **17:** 2645–54.
Kohn, W.D., Monera, O.D., Kay, C.M., and Hodges, R.S. 1995. The effects of interhelical electrostatic repulsions between glutamic acid residues in controlling the dimerization and stability of two-stranded α-helical coiled-coils. *J. Biol. Chem.* **270:** 25495–506.
Kohn, W.D., Kay, C.M., and Hodges, R.S. 1997. Salt effects on protein stability: Two-stranded α-helical coiled-coils containing inter- or intrahelical ion pairs. *J. Mol. Biol.* **267:** 1039–52.
Kriwacki, R.W., Hengst, L., Tennant, L., Reed, S.I., and Wright, P.E. 1996. Structural studies of p21Waf1/Cip1/Sdi1 in the free and Cdk2-bound state: Conformational disorder mediates binding diversity. *Proc. Natl. Acad. Sci.* **93:** 11504–9.
Kruman, I.I., Nath, A., Maragos, W.F., Chan, S.L., Jones, M., Rangnekar, V.M., Jakel, R.J., and Mattson, M.P. 1999. Evidence that Par-4 participates in the pathogenesis of HIV encephalitis. *Am. J. Pathol.* **155:** 39–46.
Krylov, D., Mikhailenko, I., and Vinson, C. 1994. A thermodynamic scale for leucine zipper stability and dimerization specificity: e and g interhelical interactions. *EMBO J.* **13:** 2849–61.
Krylov, D., Barchi, J., and Vinson, C. 1998. Inter-helical interactions in the leucine zipper coiled coil dimer: pH and salt dependence of coupling energy between charged amino acids. *J. Mol. Biol.* **279:** 959–72.
Kussie, P.H., Gorina, S., Marechal, V., Elenbaas, B., Moreau, J., Levine, A.J., and Pavletich, N.P. 1996. Structure of the MDM2 oncoprotein bound to the p53 tumor suppressor transactivation domain. *Science* **274:** 948–53.
Lavigne, P., Kondejewski, L.H., Houston Jr., M.E., Sonnichsen, F.D., Lix, B., Sykes, B.D., Hodges, R.S., and Kay, C.M. 1995. Preferential heterodimeric parallel coiled-coil formation by synthetic Max and c-Myc leucine zippers: A description of putative electrostatic interactions responsible for the specificity of heterodimerization. *J. Mol. Biol.* **254:** 505–20.
Lavigne, P., Sonnichsen, F.D., Kay, C.M., and Hodges, R.S. 1996. Interhelical salt bridges, coiled-coil stability, and specificity of dimerization. *Science* **271:** 1136–8.
Lavigne, P., Crump, M.P., Gagne, S.M., Hodges, R.S., Kay, C.M., and Sykes, B.D. 1998. Insights into the mechanism of heterodimerization from the 1H-NMR solution structure of the c-Myc-Max heterodimeric leucine zipper. *J. Mol. Biol.* **281:** 165–81.
Leberman, R. and Soper, A.K. 1995. Effect of high-salt concentrations on water structure. *Nature* **378:** 364–366.
Lumb, K.J. and Kim, P.S. 1995a. A buried polar interaction imparts structural uniqueness in a designed heterodimeric coiled coil [published erratum appears in *Biochemistry* 1998 **37:** 13042]. *Biochemistry* **34:** 8642–8.
Lumb, K.J. and Kim, P.S. 1995b. Measurement of interhelical electrostatic interactions in the GCN4 leucine zipper. *Science* **268:** 436–439.
Lupas, A. 1996. Coiled coils: New structures and new functions. *Trends Biochem. Sci.* **21:** 375–82.
Lupas, A. 1997. Predicting coiled-coil regions in proteins. *Curr. Opin. Struct. Biol.* **7:** 388–93.
Marky, L.A. and Breslauer, K.J. 1987. Calculating thermodynamic data for transitions of any molecularity from equilibrium melting curves. *Biopolymers* **26:** 1601–20.
Marti, D.N., Jelesarov, I., and Bosshard, H.R. 2000. Interhelical ion pairing in coiled coils: Solution structure of a heterodimeric leucine zipper and determination of pKa values of Glu side chains. *Biochemistry* **39:** 12804–18.
Matsuyama, S. and Reed, J.C. 2000. Mitochondria-dependent apoptosis and cellular pH regulation. *Cell Death Differ.* **7:** 1155–65.
Mattson, M.P., Duan, W., Chan, S.L., and Camandola, S. 1999. Par-4: An emerging pivotal player in neuronal apoptosis and neurodegenerative disorders. *J. Mol. Neurosci.* **13:** 17–30.
Muhle-Goll, C., Gibson, T., Schuck, P., Schubert, D., Nalis, D., Nilges, M., and Pastore, A. 1994. The dimerization stability of the HLH-LZ transcription protein family is modulated by the leucine zippers: A CD and NMR study of TFEB and c-Myc. *Biochemistry* **33:** 11296–306.
Nalca, A., Qiu, S.G., El-Guendy, N., Krishnan, S., and Rangnekar, V.M. 1999. Oncogenic Ras sensitizes cells to apoptosis by Par-4. *J. Biol. Chem.* **274:** 29976–83.
O'Neil, K.T. and DeGrado, W.F. 1990. A thermodynamic scale for the helix-forming tendencies of the commonly occurring amino acids [published erratum appears in *Science* 1991 **253:** 952]. *Science* **250:** 646–51.
O'Shea, E.K., Rutkowski, R., Stafford, 3rd, W.F., and Kim, P.S. 1989. Preferential heterodimer formation by isolated leucine zippers from fos and jun. *Science* **245:** 646–8.
Ozeki, S., Kato, T., Holtzer, M.E., and Holtzer, A. 1991. The kinetics of chain exchange in two-chain coiled coils: α α- and β β-tropomyosin. *Biopolymers* **31:** 957–66.
Page, G., Kogel, D., Rangnekar, V., and Scheidtmann, K.H. 1999. Interaction partners of Dlk/ZIP kinase: Co-expression of Dlk/ZIP kinase and Par-4 results in cytoplasmic retention and apoptosis. *Oncogene* **18:** 7265–73.
Pavletich, N.P. 1999. Mechanisms of cyclin-dependent kinase regulation: Structures of Cdks, their cyclin activators, and Cip and INK4 inhibitors. *J. Mol. Biol.* **287:** 821–8.
Pedersen, W.A., Luo, H., Kruman, I., Kasarskis, E., and Mattson, M.P. 1999. Involvement of the prostate apoptosis response-4 (Par-4) protein in motor neuron degeneration in ALS. *Soc. Neurosci. Abst.* **25:** 49.
Potekhin, S.A., Medvedkin, V.N., Kashparov, I.A., and Venyaminov, S. 1994. Synthesis and properties of the peptide corresponding to the mutant form of the leucine zipper of the transcriptional activator GCN4 from yeast. *Protein Eng.* **7:** 1097–101.
Puglisi, J.D., Chen, L., Blanchard, S., and Frankel, A.D. 1995. Solution structure of a bovine immunodeficiency virus Tat-TAR peptide-RNA complex. *Science* **270:** 1200–3.
Qiu, G., Ahmed, M., Sells, S.F., Mohiuddin, M., Weinstein, M.H., and Rangnekar, V.M. 1999a. Mutually exclusive expression patterns of Bcl-2 and Par-4 in human prostate tumors consistent with down-regulation of Bcl-2 by Par-4. *Oncogene* **18:** 623–31.
Qiu, S.G., Krishnan, S., el-Guendy, N., and Rangnekar, V.M. 1999b. Negative regulation of Par-4 by oncogenic Ras is essential for cellular transformation. *Oncogene* **18:** 7115–23.
Radhakrishnan, I., Perez-Alvarado, G.C., Parker, D., Dyson, H.J., Montminy, M.R., and Wright, P.E. 1997. Solution structure of the KIX domain of CBP bound to the transactivation domain of CREB: A model for activator:coactivator interactions. *Cell* **91:** 741–52.
Radhakrishnan, I., Perez-Alvarado, G.C., Dyson, H.J., and Wright, P.E. 1998. Conformational preferences in the Ser133-phosphorylated and non-phosphorylated forms of the kinase inducible transactivation domain of CREB. *FEBS Lett.* **430:** 317–22.
Sanchez, P., De Carcer, G., Sandoval, I.V., Moscat, J., and Diaz-Meco, M.T. 1998. Localization of atypical protein kinase C isoforms into lysosome-targeted endosomes through interaction with p62. *Mol. Cell. Biol.* **18:** 3069–80.
Saudek, V., Pasley, H.S., Gibson, T., Gausepohl, H., Frank, R., and Pastore, A. 1991. Solution structure of the basic region from the transcriptional activator GCN4. *Biochemistry* **30:** 1310–7.
Seerama, N. and Woody, R. 1993. A self-consistent method for the analysis of protein secondary structure from circular dichroism. *Anal. Biochem.* **209:** 32–44.

Sells, S.F., Wood Jr., D.P., Joshi-Barve, S.S., Muthukumar, S., Jacob, R.J., Crist, S.A., Humphreys, S., and Rangnekar, V.M. 1994. Commonality of the gene programs induced by effectors of apoptosis in androgen-dependent and -independent prostate cells. *Cell Growth Differ.* **5:** 457–66.

Sells, S.F., Han, S.S., Muthukkumar, S., Maddiwar, N., Johnstone, R., Boghaert, E., Gillis, D., Liu, G., Nair, P., Monnig, S., Collini, P., Mattson, M.P., Sukhatme, V.P., Zimmer, S.G., Wood Jr., D.P., McRoberts, J.W., Shi, Y., and Rangnekar, V.M. 1997. Expression and function of the leucine zipper protein Par-4 in apoptosis. *Mol. Cell. Biol.* **17:** 3823–32.

Sosnick, T.R., Jackson, S., Wilk, R.R., Englander, S.W., and DeGrado, W.F. 1996. The role of helix formation in the folding of a fully α-helical coiled coil. *Proteins* **24:** 427–32.

Spek, E.J., Bui, A.H., Lu, M., and Kallenbach, N.R. 1998. Surface salt bridges stabilize the GCN4 leucine zipper. *Protein Sci.* **7:** 2431–7.

Tan, R. and Frankel, A.D. 1994. Costabilization of peptide and RNA structure in an HIV Rev peptide-RRE complex. *Biochemistry* **33:** 14579–85.

Uversky, V.N., Gillespie, J.R., and Fink, A.L. 2000. Why are "natively unfolded" proteins unstructured under physiologic conditions? *Proteins* **41:** 415–27.

Weissenhorn, W., Dessen, A., Harrison, S.C., Skehel, J.J., and Wiley, D.C. 1997. Atomic structure of the ectodomain from HIV-1 gp41. *Nature* **387:** 426–30.

Wendt, H., Berger, C., Baici, A., Thomas, R.M., and Bosshard, H.R. 1995. Kinetics of folding of leucine zipper domains. *Biochemistry* **34:** 4097–107.

Wendt, H., Leder, L., Harma, H., Jelesarov, I., Baici, A., and Bosshard, H.R. 1997. Very rapid, ionic strength-dependent association and folding of a heterodimeric leucine zipper. *Biochemistry* **36:** 204–13.

Wolf, E., Kim, P.S., and Berger, B. 1997. MultiCoil: A program for predicting two- and three-stranded coiled coils. *Protein Sci.* **6:** 1179–89.

Wright, P.E. and Dyson, H.J. 1999. Intrinsically unstructured proteins: re-assessing the protein structure-function paradigm. *J. Mol. Biol.* **293:** 321–31.

Yang, A.S., Gunner, M.R., Sampogna, R., Sharp, K., and Honig, B. 1993. On the calculation of pKas in proteins. *Proteins* **15:** 252–65.

Zeng, X., Herndon, A.M., and Hu, J.C. 1997. Buried asparagines determine the dimerization specificities of leucine zipper mutants. *Proc. Natl. Acad. Sci.* **94:** 3673–8.

Zhang, Z. and DuBois, R.N. 2000. Par-4, a proapoptotic gene, is regulated by NSAIDs in human colon carcinoma cells. *Gastroenterology* **118:** 1012–7.

Zhou, N.E., Kay, C.M., and Hodges, R.S. 1994. The role of interhelical ionic interactions in controlling protein folding and stability. De novo designed synthetic two-stranded α-helical coiled-coils. *J. Mol. Biol.* **237:** 500–12.

Zitzewitz, J.A., Bilsel, O., Luo, J., Jones, B.E., and Matthews, C.R. 1995. Probing the folding mechanism of a leucine zipper peptide by stopped-flow circular dichroism spectroscopy. *Biochemistry* **34:** 12812–9.